Rev. Adv. Mater. Sci. 32 (2012) 12-18

MORPHOLOGICAL STUDY OF SnSb/GRAPHITE COMPOSITES INFLUENCED BY DIFFERENT RATIO OF Sn:Sb

Kanyaporn Adpakpang[1,2], Thapanee Sarakonsri[1,2,3], Katerina E. Aifantis[3] and Stephen A. Hackney[3,4]

[1]Center of Excellence for Innovation in Chemistry, Chiang Mai University, Chiang Mai 50200, Thailand
[2]Materials Science Research Center, Faculty of Science, Chiang Mai University, Chiang Mai 50200, Thailand
[3]Lab of Mechanics and Materials, Aristotle University, Thessaloniki 54124, Greece
[4]Materials Science and Engineering, Michigan Technological University, Houghton 49931, USA

Received: February 27, 2012

Abstract. Experimental studies have shown that Sn/graphite nanocomposites are promising anodes for next generation rechargeable Li-ion batteries, as the graphite limits the volume expansions that Sn experiences upon Li-insertion. In order to provide further mechanical stability to the Sn a fabrication methods is described that allows for SnSb alloy in addition to pure Sn to attach on graphite matrices. In order to obtain an appropriate microstructure, in which the metal islands are dispersed equally throughout the matrix, the amount of Sn used in the reaction was varied between 10-40% while the Sb content was retained at 10%. Also to examine substrate effects three different graphites (artificial graphite, natural graphite and MCMB graphite) were used. The experimental process was carried out under the solution route in which $NaBH_4$ and ethylene glycol were used as the reducing agent and solvent, respectively. Performing X-ray diffraction and electron microscopy revealed that the preferred SnSb phase with ratio Sn:Sb of 1:1 was obtained when the weight of the reactants was 10 wt.% of Sb, 20 wt.% of Sn, and 70 wt.% of artificial graphite.

1. INTRODUCTION

Since Li-ion batteries are the main energy source is various portable electronic applications, significant focus in given on increasing their capacity. One way to achieve this is to replace graphitic anodes (which are used commercially since the first generation of lithium ion batteries was invented by Sony in 1990s [1]) with metal-based anode materials that allow for higher capacities. The most promising such materials are Si, Sn, and Sb due to their high charge-discharge capacity of 4200, 996, and 660 $mAhg^{-1}$, respectively [2-3] as opposed to 372 mAh/g provided by graphite. Upon Li-insertion, however, these metals experience severe volume expansion up to 300~400% [2], and therefore fracture and capacity fade occurs. To alleviate these volume expansions, Si, Sn, and Sb are attached or embedded in a matrix [4-10] that can provide mechanical stability. Another method to control the structural expansion is to allow the metal-based anodes to have an intermetallic or multiphase form, since different metals react at different voltages. Therefore, the anode structure expands stepwise leading to cycling stability by its smooth volume expansion.

A most common intermetallic anode studied is that comprised of Sn and Sb based alloys and composites fabricated with using various methods such as mechanical alloying, co-precipitation, reduction, sol-gel, microwave, *etc*. [11-18]. Among

Corresponding author: Thapanee Sarakonsri, e-mail: tsarakonsri@gmail.com

them, the solution method is widely used due to its simplicity and inexpensiveness. The most important factor is that the solution method provides a very small particle size for the end products, as reported on the preparation of CNTs-Sb [19], CNTs-$SnSb_{0.5}$ [19], Sn-SnSb/graphite [20], Sn/SnSb [21,22], and SnSb/graphite [23] nanocomposites. However, the preparation of these materials was carried out for more than one step. To facilitate the material fabrication, we accomplished the preparation of SnSb/graphite composites in one step by an uncomplicated solution process, which has not been reported in previous studies. The intermetallic structure and graphite matrix will allow for mechanical stability upon Li-insertion.

2. EXPERIMENTAL DETAILS

The technique employed for fabricating SnSb/graphite composites is the solution method. $SnCl_2 \cdot H_2O$ (Fluka, 99.99%), anhydrous $SbCl_3$ (Aldrich, 99%), were as used as the metal ion precursors, while natural graphite (NG), artificial (AG), and mesocarbonmicrobead (MCMB) graphites were used as the carbon precursors. $NaBH_4$ (Merck, >96%) and ethylene glycol (J.T. Baker, 99.9%) were used as the reducing agent and solvent, respectively. The procedure was to firstly dissolve anhydrous $SbCl_3$, and then $SnCl_2 \cdot H_2O$ in in 100 ml of deoxygenated ethylene glycol (by N_2 gas) followed by adding graphite powder (AG, NG or MCMB) after the metal salts were completely dissolved. After that, the solution was sonicated for 30 minutes, and sodium borohydride was added. The reaction was carried out under nitrogen atmosphere and the reaction time was 10 minutes after the reducing process. Precipitate from the solution was collected by centrifugation which later dried in an oven at 70 °C for 2 hours. The compositions of the solutions will be described in terms of weight percentages calculated by dividing the weight of the metal or carbon added to solution by the weight of the metal plus carbon. In each condition, the weight percentage of Sn metal added was fixed as 10% while the types of graphite and weight percentage of Sn were varied as show in Table 1.

All preparative samples were characterized by X-ray diffraction (XRD) using a Bruker AXS D8 diffractometer (Cu K_α (λ = 1.54 Å) Ni filter, 2θ = 10-80° with a scan rate of 0.04 degrees per second for phase identification. Transmission electron microscopy (TEM, JEOL JEM-2010) was used for analyzing the product morphology and particle size. Moreover, the elemental composition and metal dispersion were characterized by scanning electron microscopy (SEM, JEOL JSM-5910LV) equipped with energy dispersive spectroscopy (EDS, INCA-The Microanalysis Suite Issue 16).

3. RESULTS AND DISCUSSION

The study of phase formation by using XRD technique shows that SnSb phase occurred, and matched with JCPDS file no.33-0118, incorporated with graphite (JCPDS file no.1-0640) in all preparative conditions. The XRD patterns of the resulting products are shown in Figs. 1 and 2, respectively. All SnSb/C samples contained SnSn intermetallic compound, while increasing the Sn content above 1:1 Sn:Sb by weight, resulted in the formation pure Sn phase as well (JCPDS file no.1-0926) as shown in Figs. 2a and 2b, respectively.

Reaction 1 illustrates the reaction by which the formation of SnSb phase occurred on graphite un-

Table 1. Preparative codes and details of the prepared samples.

Sample	%Sb	%Sn	Types of graphite
1	10	10	Artificial (AG)
2	10	20	Artificial (AG)
3	10	30	Artificial (AG)
4	10	40	Artificial (AG)
5	10	10	Mesocarbonmicrobead (MCMB)
6	10	20	Mesocarbonmicrobead(MCMB)
7	10	30	Mesocarbonmicrobead(MCMB)
8	10	40	Mesocarbonmicrobead(MCMB)
9	10	10	Natural (NG)
10	10	20	Natural (NG)
11	10	30	Natural (NG)
12	10	40	Natural(NG)

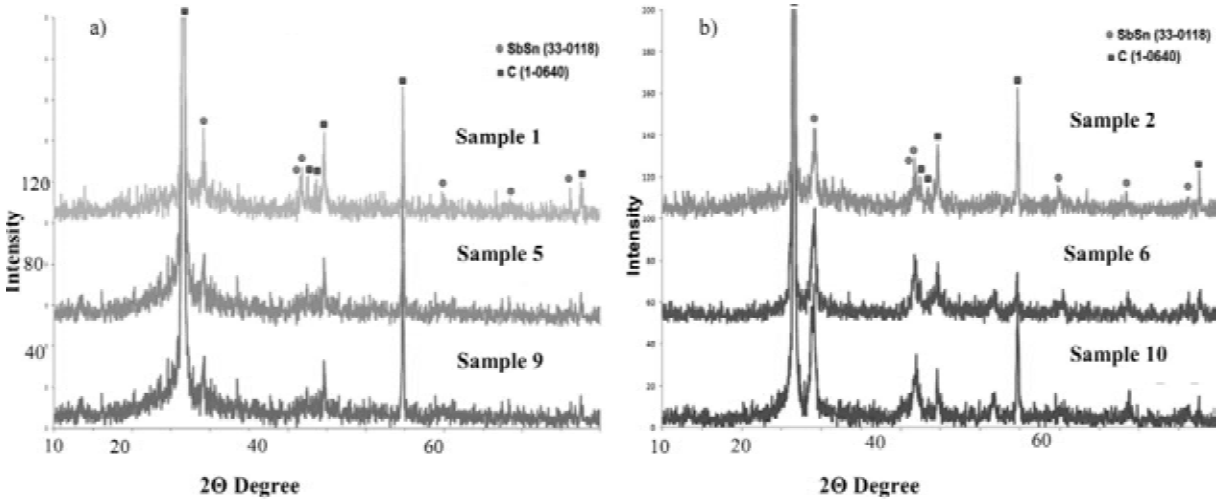

Fig. 1. (a) XRD patterns 10% Sb-10% Sn on graphite AG, MCMB, and NG (samples 1, 5, 9), (b) XRD patterns10% Sb-20% Snon graphite AG, MCMB, and NG (samples 2, 6, 10).

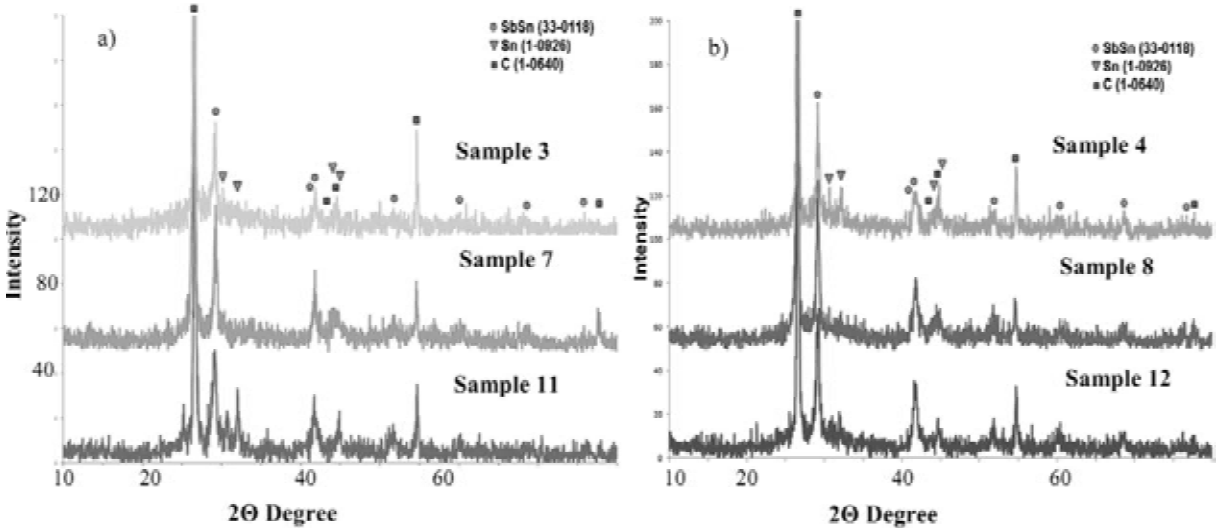

Fig. 2. (a) XRD patterns10% Sb-30% Sn on graphite AG, MCMB, and NG (samples 3, 7, 11), (b) XRD patterns10% Sb-40% Sn on graphite AG, MCMB, and NG (samples 4, 8, 12).

der the reducing process of $NaBH_4$when ethylene glycol was used as the solvent. It is proposed that BH_4 – a high power reducing agent ($E°$ = -1.24) – donated electrons to Sn^{2+} (Sn^{2+}/Sn, $E°$ = -0.14) and Sb^{3+} (Sb^{3+}/Sb, $E°$ = 2.0) cations to form SnSb on the graphite surface. During the reaction, $BH_4$with four H-B bonds, and four H-O bonds from two molecules of ethylene glycol were broken.

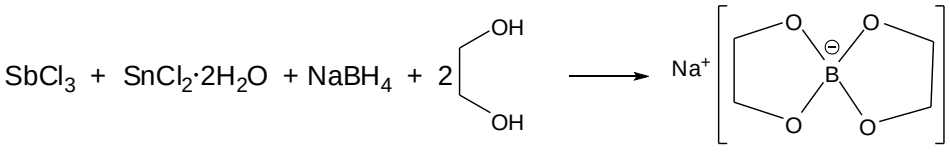

, (1)

$$+ \ 5HCl \ + 3/2H_2 \ + 2H_2O + SnSb$$

Then, cyclic chelate structure took place based on the alcoholysis of BH_4 (reaction 2) which can occur fast at room temperature [24].

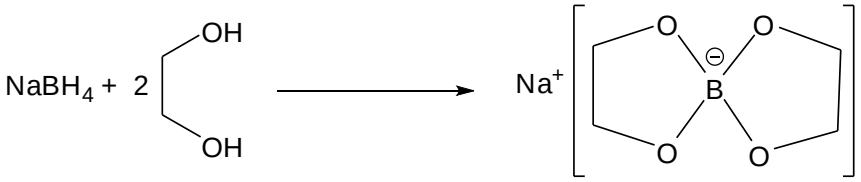

, (2)

Apart from the formation of SnSb phase, Sn pure phase was observed in some preparative conditions in which wt.% of Sn was augmented to 30 and 40 wt.% The formation of Sn phase was possibly caused by the inadequate amount of Sb^{3+} in the system to form SnSb, thus, the excess amount of Sn^{2+} took electrons from borohydride and then formed Sn pure phase as indicated in reaction 3.

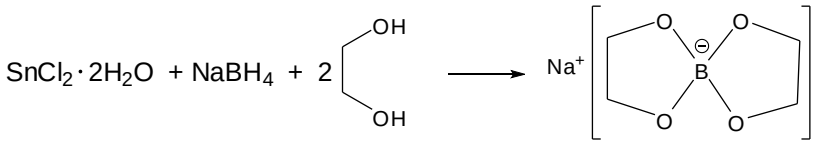

(3)

$$+ \ 2HCl \ + 3H_2 \ + 2H_2O + Sn$$

The elemental composition of all samples was measured by using SEM-EDS. To clarify in a comparative way, the samples were distinguished in a group of wt.% of Sb:Sn on several graphite types as shown in Table 2. The elemental wt.% indicated in Table 2 was the average value detected randomly from five areas of each sample. The results agreed well with the XRD spectrum which indicated that both Sb and Sn crystal structures were present. For lower %wt of Sn where the atomic ratio of Sb to Sn was nearly 1:1, only SbSn phase formed. Increasing the %wt of Sn in solution to 30 and 40%wt, the atomic ratio of Sn:Sb in solution was increased from 1.5 to 2 led to increased amounts of the metallic Sn phase (XRD patterns for samples 11 and 4 in Figs 2a and 2b).

The dispersion of SnSb on the carbon surfaces was studied by Back-scattered electron contrast (BEC) technique. SnSb and Sn appeared as bright areas dispersed on graphite. Rectangular areas are used to

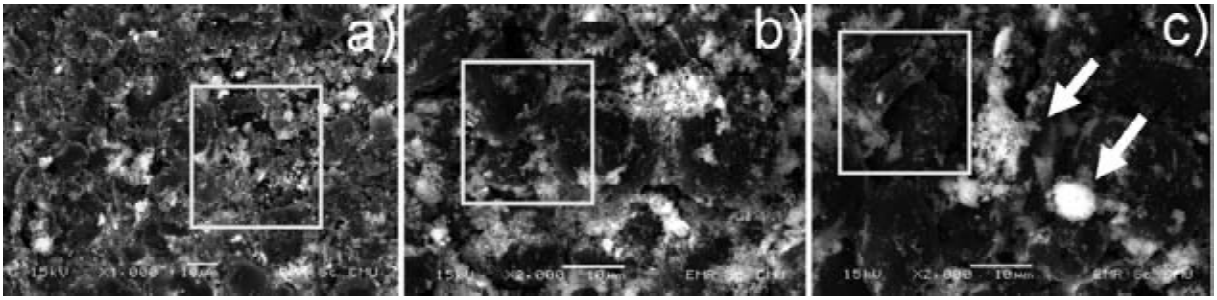

Fig. 3. Back-scattered electron images of: (a) sample 1, (b) sample 5, and (c) sample 9. The scale bars are 10 microns.

Table 2. Elemental measurement by EDS technique for samples varied Sb:Sn as 10:10, 10:20, 10:30, and 10:40 wt.%.

Sample	Elements (wt.%)				Sb:Sn
	Sb	Sn	C	O	
1	18.17	10.61	62.61	8.62	1 : 0.6
5	14.71	10.09	66.30	8.91	1 : 0.7
9	21.12	10.34	60.05	8.39	1 : 0.5
2	10.48	9.40	69.81	10.31	1 : 0.9
6	8.58	6.73	69.25	15.43	1 : 0.8
10	19.55	15.36	53.09	12.00	1 : 0.8
3	10.91	12.78	59.28	17.04	1 : 1.2
7	11.18	21.45	46.13	21.25	1 : 2.0
11	10.36	27.36	51.70	10.58	1 : 2.7
4	14.44	23.36	48.95	13.26	1 : 1.7
8	13.22	17.25	56.57	12.95	1 : 1.3
12	19.32	26.67	39.22	14.78	1 : 1.4

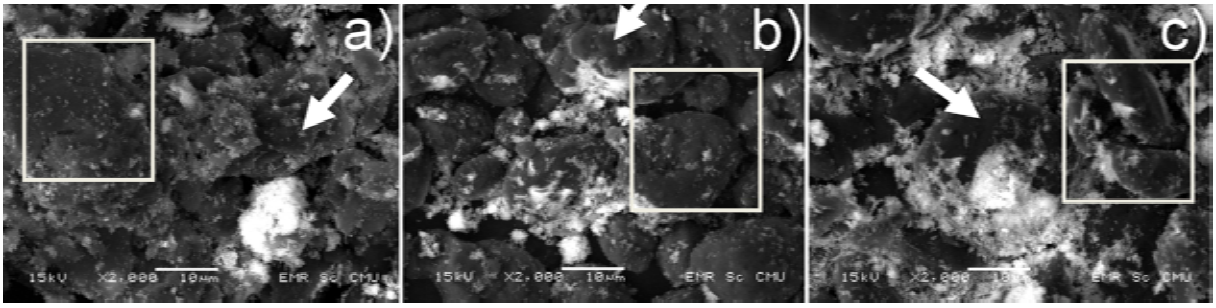

Fig. 4. Back-scattered electron images of: (a) sample 2, (b) sample 6, and (c) sample 10.

depict areas containing smaller particles, while larger particles are indicated by arrows (Figs 3 and 4). The ratio of Sb:Sn deposited for samples 3 and 4, was slightly less than 1:1 where the wt. % of Sn for the solution was 10% and 20% respectively (Table 2). For sample 1 in Fig. 3, although the SbSn phase had a good dispersion on graphite (depicted in the rectangular area), there were some large SnSb islands. Such a microstructure is not appropriate for anode materials. Furthermore, numerous large islands formed when the amount of Sn for the solution was increased to 30 and 40% (Figs. 5 and 6) and the ratio of Sb:Sn was 1:*X* (*x*=1.5-2). As the Sn amount increased, the degree of agglomeration also increased. This phenomenon resulted by the large surface area of Sn particles, which resulted in an aggregation of Sn and also the formation of larger Sn islands [10,25]. Similarly, with the increase in Sn content, the SnSb particles also increased in diameter. The above agglomerates can be explained by the graphite amount contained in the samples. When the ratio of Sb:Sn was varied as 10:10 wt.% for the solution, the amount of graphite was 80 wt.%. This large amount of graphite provided abundant surface area for SnSb nucleates to be deposited. However, as the Sn was increased to 20, 30, and 40 wt.%, the graphite amount was decreased as 70, 60, and 50 wt.%, respectively (Table 3). The relationship between particle size and wt% garphite is rationalized by considering that as more SnSb material formed on less graphite surface area, the volume of metal is accumulated in fewer, but larger particles.

The TEM images (Fig. 7) agreed with the BEC images. When the Sn content was low SnSb small particles loosely aggregated (Fig. 7a). When the Sn content increased above 30 wt.%, the SnSb particles aggregated tightly forming large islands and also larger particles (Figs. 7b and 7c). From all experimental evidences, it can be concluded that

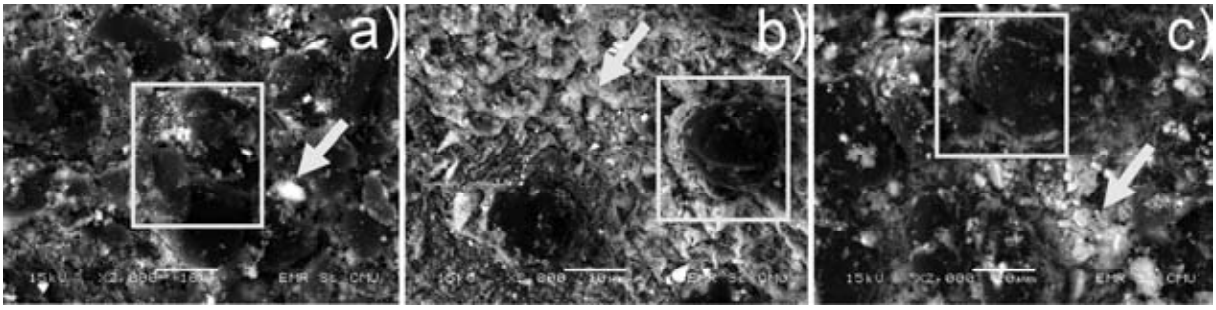

Fig. 5 Back-scattered electron images of: (a) sample3, (b) sample 7, and (c) sample 11.

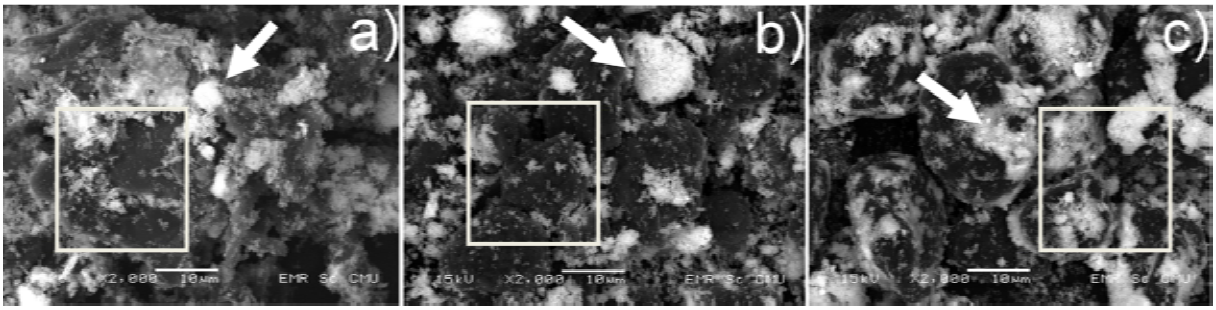

Fig. 6. Back-scattered electron images of: (a) sample 4, (b) sample 8, and (c) sample 12.

Table 3. Group of samplesdescribing wt.% of graphite contained.

Group	Samples	%Sb	%Sn	%graphite
1	1,5,9	10	10	80
2	2,6,10	10	20	70
3	3,7,11	10	30	60
4	4,9,12	10	40	50

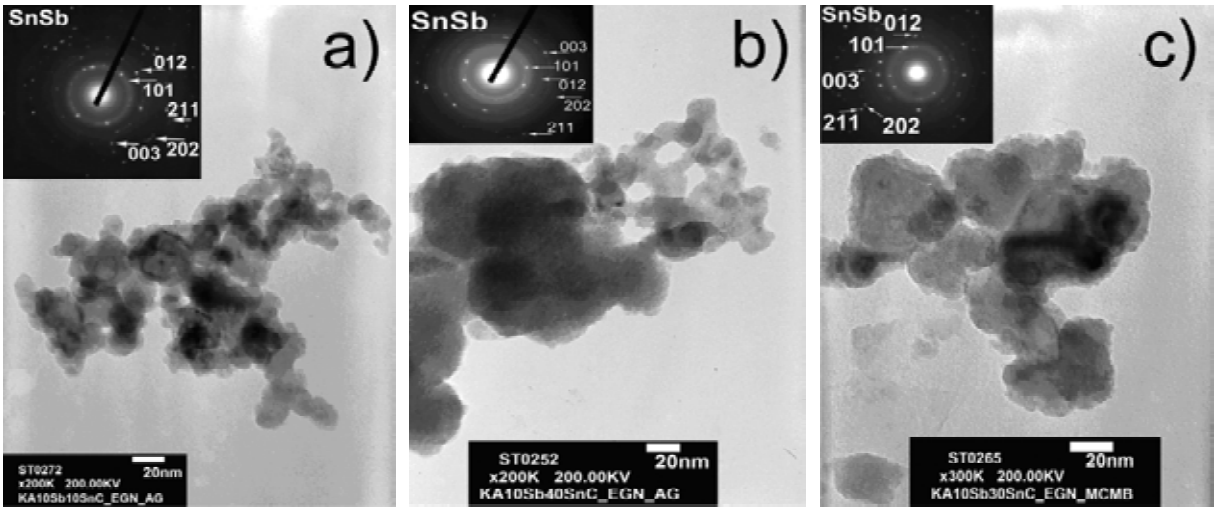

Fig. 7. Bright-field TEM micrographs inserted with Selected-area electron diffraction (SAED) patterns of: (a) sample10, (b) sample 4, and (c), sample 7.

the amount of Sn added in samples played an important role for the particle size of the SnSb phase. The amount and types of graphite matrix mainly influenced the dispersion behavior of the SnSb alloy.

4. CONCLUSIONS

SbSn-graphite composites were successfully prepared using the solution methord. The wt.% of the Sb for the solution was kept at 10%, while the Sn content for the solution was varied from 10-40 wt.%, resulting in a variable graphite content. SbSn phase was observed in all end products, while for Sn contents greater than 30 wt.%, pure Sn phase was also attached on the graphite. Increasing the Sn content allowed for a greater amount of Sn and SnSb to attach on the graphite, while the available graphite was reduced. This resulted in agglomeration anf therefore the Sn and SnSb islands were in the micron-scale. Using 10 wt.% of Sb, 20 wt.% of Sn with artificial graphite allowed for the best microstructure for anodes, since a uniform distribution of SnSb nanoparticles on graphite was obtained and the Sn:Sb ratio was 1:1, allowing for all Sn to be alloyed with the Sb.

ACKNOWLEDGEMENTS

KA and TS are very grateful to the Center of Excellence for Innovation in Chemistry (PERCH-CIC), Materials Science Research Center, and National Research University (NRU) Project of Thailand for financial support. Department of Chemistry, Chiang Mai University was also acknowledged for laboratory and product characterization facilities. KEA, TS and SAH are grateful to the European Research Council Starting Grant 211166 MINATRAN.

REFERENCES

[1] T. Nagaura and K. Tozawa // *Prog. Batt.Solar Cells* **9** (1990) 209.
[2] L.Y. Beaulieu, K.W. Eberman, R.L. Turner, L.J. Krause and J.R. Dahn // *Electrochem. Solid-State Lett.* **4** (2001) A137.
[3] A. Trifonova, M. Wachtler, M. Winter and J.O. Besenhard // *Ionics* **8** (2002) 323.
[4] Y. Zhang, X.G. Zhang, H.L. Zhang, Z.G. Zhao, F. Li, C. Liu and H.M. Cheng // *Electrochimica Acta* **51** (2006) 4994.
[5] J. Park, J. Eom and H. Kwon // *Electrochem. Commun*. **11** (2009) 596.

[6] F. Nobili, M. Mancini, S. Dsoke, R. Tossici and R. Marassi // *J. Power Sources* **195** (2010) 7090.
[7] J. Chen, L. Yang, S. Fang and S. Hirano // *Electrochem. Commun*. **13** (2011) 848.
[8] L. Balan, J. Ghanbaja, P. Willmann and D. Billaud // *Carbon* **43** (2005) 2311.
[9] C.M. Park and H.J. Sohn // *Electrochimica Acta* **54** (2009) 6367.
[10] K.E. Aifantis, T. Huang, S.A. Hackney, T.Sarakonsri and A. Yu // *J. Power Source* **197** (2012) 246.
[11] H.Guo, H. Zhao, C. Yin and W.Qiu // *J. Alloys Compd*. **426** (2006) 277.
[12] J. Yang and J.I. Wang, *Negative Electrodes: Lithium Alloys* (Elsevier, Amsterdam, 2009), p.225.
[13] M.S. Park, S.A. Needham, G.X. Wang, Y.M. Kang, S.J. Park, S.X. Dou and H.K. Liu // *Chem. Mater*. **19** (2007) 2406.
[14] H. Li, Q. Wang, L. Shi, L. Chem and X. Huang // *Chem. Mater*. **14** (2002) 103.
[15] J.H. Kim, G.J. Jeong, Y.W. Kim, C.W. Park and C.K. Lee // *J. Electrochem. Soc.* **150** (2003) A1544.
[16] C. Kim, M. Noh, M. Choi, J. Cho and B. Park // *Chem. Mater*. **17** (2005) 3297.
[17] K.T. Lee, Y.S. Jung and S.M. Oh // *J. Am. Chem. Soc*. **125** (2003) 5652.
[18] M. Marcinek, L.J. Hardwick, T.J. Richardson, X. Song and R. Kostecki // *J. Power Sources* **173** (2007) 965.
[19] W.X. Chen, J.Y. Lee and Z. Liu // *Carbon* **41** (2003) 959.
[20] K.L. Huang, G. Zhang and S.Q. Liu // *Trans. Nonferrous Met. Soc. China* **17** (2007) 841.
[21] S.A. Needham, G.X. Wang and H.K. Liu // *J. Alloys Compd.* **400** (2005) 234.
[22] A. Trifonova, M. Wachtler, M.R. Wagner, H. Schroettner, C. Mitterbauer, F. Hofer, K.C. Möller, M. Winter and J.O. Besenhard // *Solid State Ion.* **168** (2004) 51.
[23] D. Billaud, C. Nabais, C. Mercier, R. Schneider and P. Willmann // *Energ. Convers. Manage*. **49** (2008) 2447.
[24] J. Zhang, T.S. Fisher, J.P. Gore, D. Hazra and P.V. Ramachandran // *Int. J. Hydrogen Energ*. **31** (2006) 2292.
[25] K.E. Aifantis, M. Haycock, P. Sanders and S.A. Hackney // *Mater. Sci. Eng.* **A529** (2011) 55.